

Supporting Information

Mechanical strain-induced wavevector switching of spin textures in a
(Fe,Ni,Pd)₃P magnet with anisotropic Dzyaloshinskii-Moriya interaction

Shunsuke Mori¹⁺, Seiichiro Ii², Taku Moronaga^{2,3}, Toru Hara^{2,3}, Kosuke Karube¹, Yasujiro
Taguchi¹, Yoshinori Tokura^{1,4,5}, Xiuzhen Yu¹

+astamuse Co., Ltd., Tokyo 101-0054, Japan

¹ RIKEN Center for Emergent Matter Science (CEMS), Wako, Saitama 351-0198, Japan

² Research Center for Structural Materials, National Institute for Materials Science (NIMS),
Tsukuba, Ibaraki 305-0047, Japan

³ Research Network and Facility Services Division, National Institute for Materials Science
(NIMS), Tsukuba, Ibaraki 305-0047, Japan

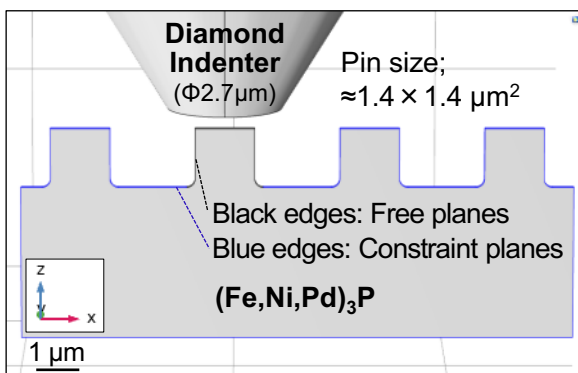
⁴ Department of Applied Physics, The University of Tokyo, Tokyo 113-8656, Japan.

⁵ Tokyo College, The University of Tokyo, Tokyo 113-8656, Japan.

1. Finite element simulations (FEM) of FNPP thin plate.

We conducted FEM simulations using COMSOL Multiphysics software. Fig. S1a is a model of the experiments showing geometry and boundary conditions. The diameter of a diamond indenter and pin size correspond to measurements from TEM images. In this model, three edges of a square pin compressed by indenter (black lines in Fig S1) are free while other edges (blue lines in Fig S1) are fixed. Accordingly, a total of 471,772 meshes are created for precise calculations around boundaries. The simulate results in Fig .1b well agree with a deformation observed by TEM images showing almost only square pins deforms under compression. The mechanical properties of a sample except for density are alternatively referred to Fe₃P.¹

a Geometry and boundary conditions



b Meshing

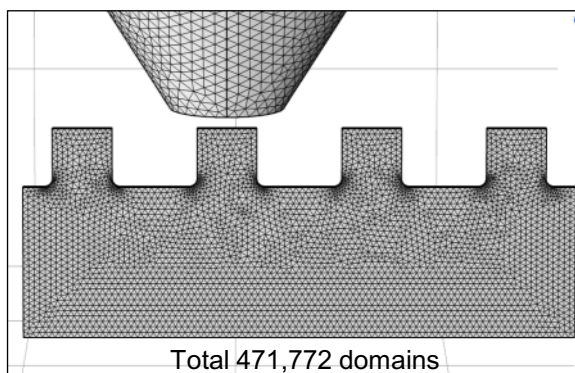
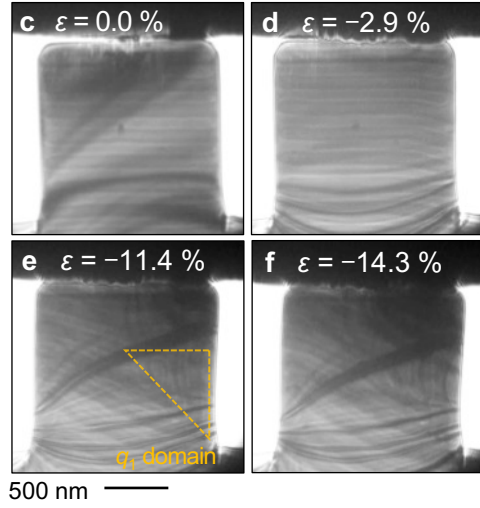
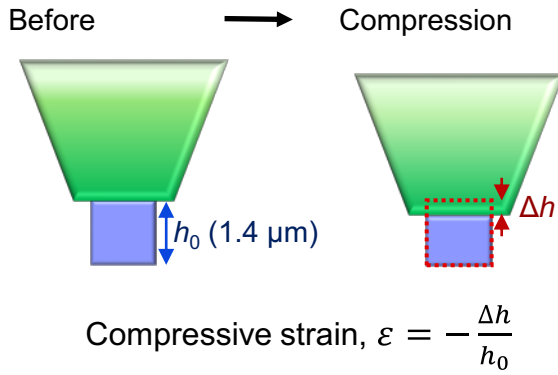


Figure S1. The model and conditions of FEM simulations

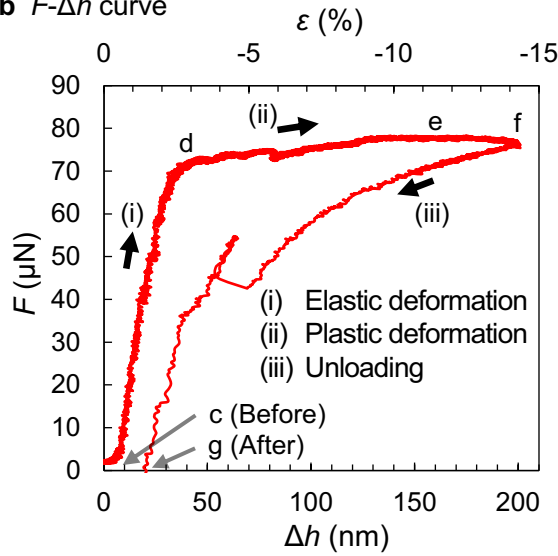
2. Schematics and representations of nanoindentation tests.

Figure S2a schematically shows the way to calculate the compressive strain, where strain (ε) is defined as $\varepsilon = -\Delta h/h_0$ according to a distance from the sample top (h) and an initial height of the sample (h_0). The force (F) was simultaneously measured during nanoindentation tests. Based on this method, we plotted $F - \Delta h$ curve with a calculated compressive strain at the upper horizontal axis. The sample fracture of each pin depends on minor differences of compressive conditions as shown in Fig. S4. $F - \Delta h$ curve in Fig. S2b shows both loading and unloading process because the sample was not broken, which is similar behavior to typical indentation curve observed in bulk samples. The displacement after unloading is around 20 nm (not zero) indicating that there is residual strain owing to plastic deformation. The L-TEM image series under uniaxial compressive strain and after unloading was displayed in Fig. S2c-g. During the elastic region (Fig. S2d), the slight bending of the magnetic stripe was observed. These bent stripes transformed into the vertical direction of q_1 domain from the right-bottom edge, which is enclosed by an orange triangle in Fig. S2e. These behaviors are well accordance with the observed results of pin 2 in the main text (Fig. 3). After reaching the maximum strain ($\varepsilon = -14.3\%$), the magnetic textures recovered to the initial state during the unloading process. However, the q_1 domain was partially stabilized after the indentation test, indicating that the residual compressive strain induced nonvolatile switching of stripe domains.

a Illustration for the calculation of strain



b $F-\Delta h$ curve



g After ($\varepsilon_{\text{res}} = -1.4 \%$)

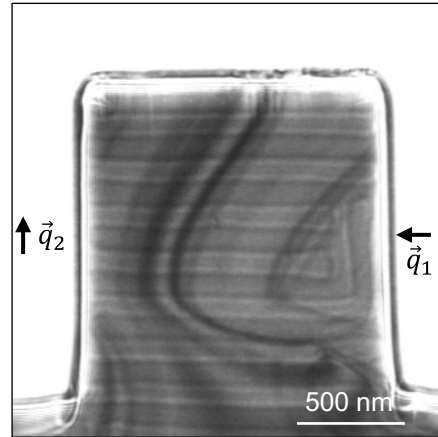


Figure S2. **a** Schematic description of the way to calculate uniaxial compressive strain. **b** The measured $F-\Delta h$ curve during indentation of pin 1. The upper horizontal axis presents corresponding uniaxial compressive strain. **c-f** The series of L-TEM image under uniaxial compressive strain. **g** The L-TEM image after unloading with residual strain.

3. Nanoindentation and a series of L-TEM image for pin 4.

We performed the nanoindentation test for pin 4. Figure S3a presents the $F - \Delta h$ curve exhibiting both loading and unloading process because the sample was not broken. The L-TEM image series under uniaxial compressive strain and after unloading was displayed in Fig. S3b-h. The q_1 domain is mainly observed at the bottom of the square, and there are negligible changes in magnetic textures. These results indicate that the q_1 domain is robust under compressive strain, which is accordance with the observed results of pin 3 in the main text (Fig. 4).

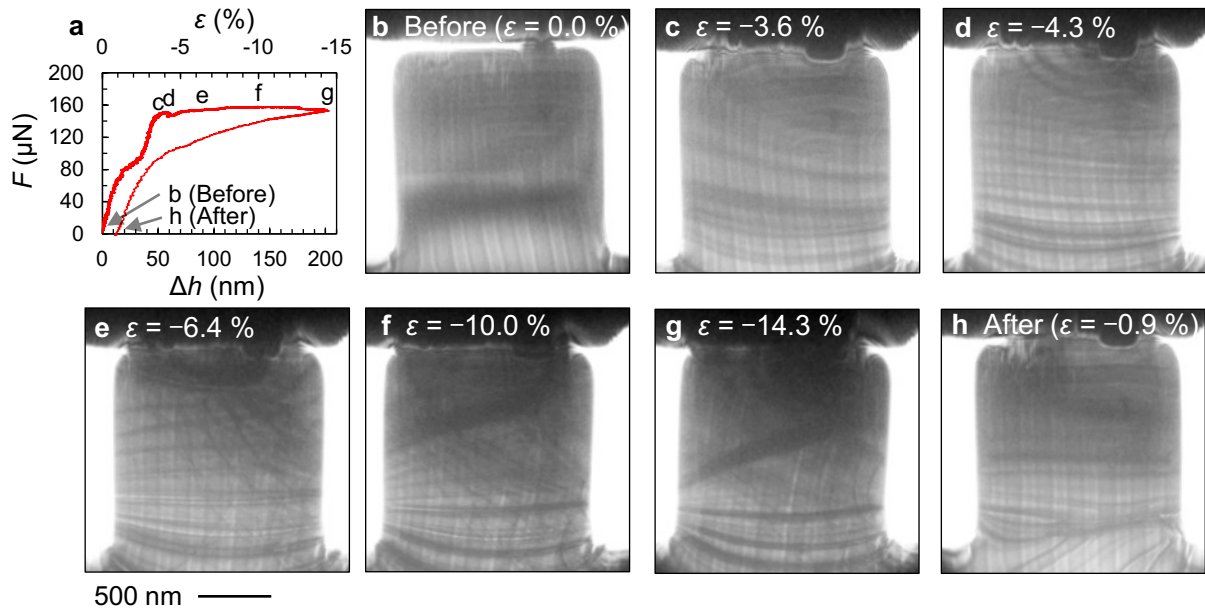


Figure S3. The results of nanoindentation test and in-situ L-TEM observations of the pin 4. **a** The measured $F - \Delta h$ curve during indentation. The upper horizontal axis presents corresponding uniaxial compressive strain. **b-g** The L-TEM image series under uniaxial compressive strain. **h** The L-TEM image after unloading with residual strain.

4. FEM simulation of deviation from uniaxial strain

Fig. S4 presents the stress distribution when the indenter and pin are not perfectly parallel each other during compression. Fig. S4a and S4b are the model and calculated stress mapping image when the indenter is tilted 0.3 degree along the length direction of FNPP. FEM simulation results indicate that the stress is concentrated at the right edge and compressive strain somewhat deviates from the uniaxial direction. This inhomogeneity is supposed to induce slight bending of magnetic stripe shown in Fig. 4 in the main text. Figures S4c and S4d are the model and calculated stress mapping image when the indenter is tilted 0.3 degree along the thickness direction of FNPP. This result indicates that the sample is largely bent along the stress direction. Such an unprecedented deformation is plausible for fractures like pin 2 and 3.

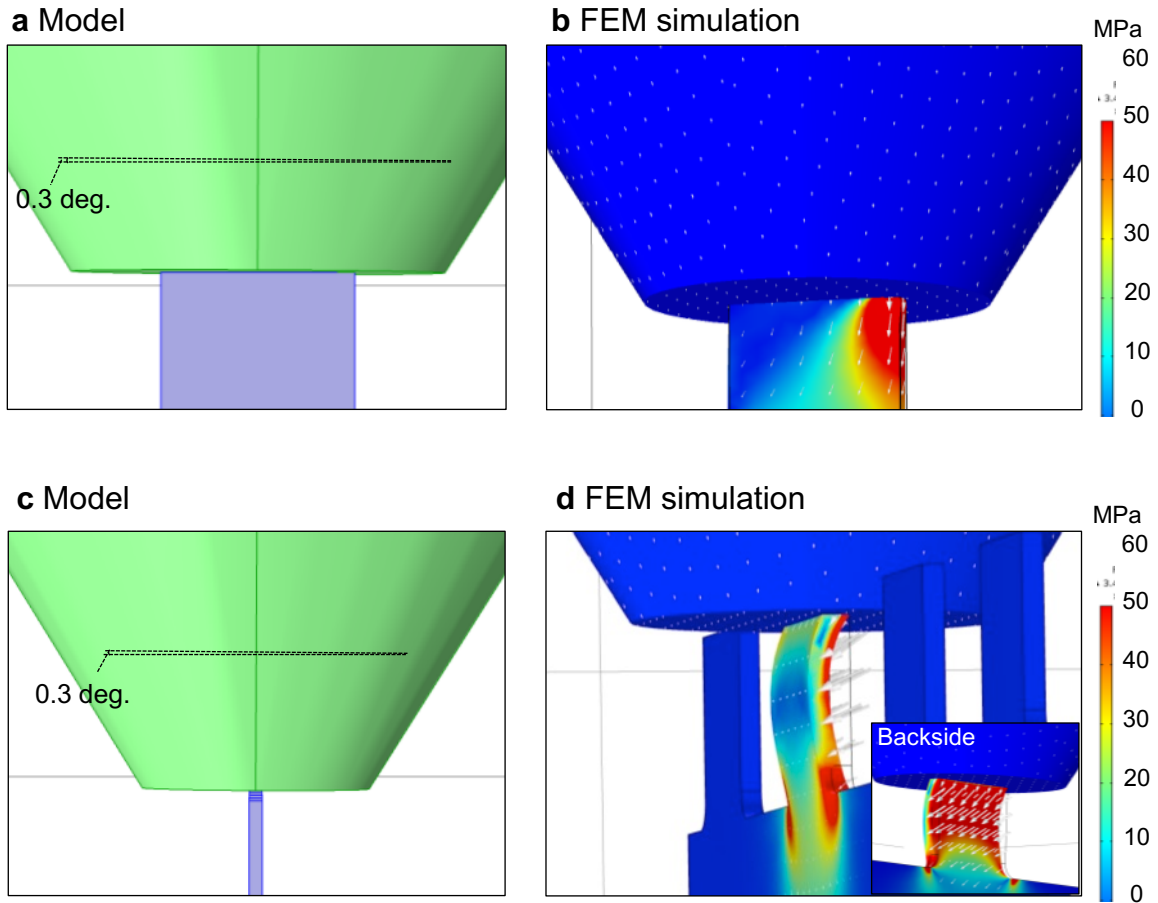


Figure S4. The simulated results of stress mapping when the indenter is not perfectly parallel to the square pin. **a,b** The model of FEM and simulated stress mapping of the pin and indenter when the indenter is tilted by 0.3 degree along the planar direction. **c,d** The model of FEM and simulated stress mapping of the pin and indenter when the indenter is tilted by 0.3 degree along the thickness direction.

REFERENCES

1. Wu, J; Chong, X.; Zhou, R.; Jiang, Y.; Feng J. Structure, stability, mechanical and electronic properties of Fe–P binary compounds by first principles calculations. RSC Adv. 5, 81943 (2015). <https://doi.org/10.1039/C5RA09875K>